Journal of Science and Technology Research

Journal homepage: www.nipesjournals.org.ng

Variation Method for Displacement and Stress Analysis of Trigonometric 3-D Shear Deformable Plate Under Distributed Lateral Loading

Festus Chukwudi Onyeka
Edo State University Uzairue, Edo Sate, 312102, Nigeria.
Email: onyeka.festus@edouniversity.edu.ng

Article Info	Abstract
  	In this work, variational calculus was applied to the analysis of stresses and displacement of a rectangular plate carrying a uniformly distributed lateral load. A 3-D trigonometric shear deformation model was developed using the elastic static principle and applied in the coupling the 3-D kinematics and constitutive relations from which the total potential energy equation was formulated. The formulated energy equation was transformed into the equilibrium equation which was used to obtain the shape function of the plate. An exact trigonometric deflection of the plate which is a product of its coefficient and shape function was obtained analytically through the principle of general variation. Furthermore, the formula for calculation of the displacements and stresses induced due to application of a lateral load in the plate was obtained by the direct variation of the total potential energy equation to produce a reliable solution for the statically bending analysis of the plate. The outcome of the numerical analysis revealed that increase in the span-thickness ratio led to the decrease in the value of displacement and stresses induced in the plate. On the other hand, as the longest-breadth ratio of the plate increased, the value of the displacement and stresses in the plate increases. The result showed that the present model developed gives distinct and satisfactory solution but still followed an identical pattern when compared with previous studies, this shows the credibility of the derived relationships. The percentage error analysis showed that the present model stress prediction for the analysis proved more reliable and can be used with confidence for the analysis of any type of rectangular plate compared to the approximate or 2-D model for the given edge condition.

1.0. Introduction

Plates are three-dimensional structural members having spatial dimensions along x, y, z-axes whose thickness is geometrically less compared to other dimensions [1-2]. They are vastly applied in aeronautical, naval, mechanical, Geotechnical and structural engineering for modelling water tanks, bridge deck slabs, turbine disks, ship hulls, retaining walls, machine parts, architectural structures [3-5]. Plates can be classified according to shapes such as; quadrilateral, square, circular or rectangular; they can be classified based on the integral constituents as homogeneous, non-homogeneous, orthotropic, anisotropic or isotropic [6-7]. Considering boundary status, plates are either fixed, free or simply supported, and they can be thin, moderately thick or thick according to their weight [8-10].

Rectangular plates a/t ≤ 20 are addressed as thick plate, while 20 ≤ a/t ≤ 50 as moderately-thick plates and 50 ≤ a/t ≤ 100 as thin plate, where a/t is the span-to-depth ratio [11]. There is increasing research interest for thick plates in engineering structures among scholars due to their pertinence and captivating attributes, features such as lightweight, heavy loads carrying-capacities, cost reduction, high mechanical properties and ability to be customized to the desired state [12]. The properties of thick plates can be improved with adequate perspicacity of its failure form and structural trait.

The investigation on thick plates can be generally and thoroughly made through bending, vibration or buckling [13-15]. The deformation of plates, due to the application of lateral loads or external forces on the plate, at right angles towards the surface of the plate is considered as a bending phenomenon. Deformation extends as the induced load exceeds the critical load [16-17]. This results to plate failure. This study is of great essence because the bending mannerism of thick plates requires adequate attention to circumvent structural instability emanating from deformations and obtain an exact solution.

Several theories such as the classical plate theory (CPT), refined plate theories (RPTs), and three-dimensional theory (3-D) [18] were formulated and deployed by diverse scholars to solve the plight of instability arising from bending. RPTs consist of FSDT [19-20], TSDT [21-22], ESDT [23], PSDT [24] and HSDT [25-26]. An accurate solution for the bending of thick plates cannot be actualized using Kirchhoff plate theory (CPT) [27] because it neglects transverse shear effects. Although RPTs give a better analytical result, their solution is incomplete and inconsistent as they overlook the normal stress and strain along the thickness axis of the plate.

The solutions of the 3D model are accurate and reliable as the limitations of 2D-RPT is terminated with the comprehensive system of fifteen governing equations which consists of material constitutive laws for generalized stress - strain equations, the kinematic relations for six strains and displacements and the three differential equations of equilibrium [28-30]. This study is needful as thick plate analysis a three-dimensional problem and it is advantageous as it investigates thick plates with SCFC support order.

Studies on bending can be carried out numerically, analytically or using an energy approach or a miscellany of any [31]. In the analytical approach, the outcome of the bending issue covers the edge requirements of the plate in the governing equations at different positions of the plate surface. This method includes; Integral transforms, Eigen expansion, Naiver and Levy series [1, 32], while the numerical approach whose solutions are approximate [33-34], consists of; Galerkin, Collocation, Bubnov-Galerkin, truncated double Fourier series, Kantorovich methods, boundary element, Ritz, and finite difference. The energy method whose total energy is equal to the sum of strain and potential energy or external work on the continuum [35]; can be in an analytical or a numerical form.

Unlike the preceding works, this study evaluates the deflection, shear stresses at the x-y axis, x-z axis and y-z axis, the normal stresses along x, y and z co-ordinates produced due to the applied load on the plate, as well as the in-plane displacement in the direction of x and y co-ordinates. Inexact solutions were obtained by past authors that employed assumed displacement-shape functions and others that used an exact process only applied it to the solution of the 2-D bending problem of the thick plate. The nature of the shape functions used during analysis matters so much to the designer as it affects the applicability and performance of the structure; to enhance the robustness of the process and at the same time ensure structural integrity and accuracy of solutions in the plate bending problem, a 3-D polynomial theory is required. This study also addresses this gap by excellently combining RPT of fourth order polynomial with a 3-D elasticity plate theory which is an improvement to past works and more advantageous as it can easily be employed to analyze plates with any boundary condition. A thick plate that is subjected to a uniformly-distributed transverse loads, and simply supported on one edge, free at one edge and clamped at the two other edges (SCFC) were evaluated herein, using a 3-D polynomial plate theory and exact polynomial

displacement function to determine value of displacements, moments and stresses along x, y and z co-ordinate at arbitrary nodes of plates.

1.1. Review of Previous Studies

Bi-directional bending investigation of thick isotropic plates was carried out by Bhaskar *et al.,* [36] using a new inverse TSDT and a finite element solution was developed, considering the effects of transverse shear deflection and rotating inertia. With the application of the dynamic version of the virtual work principle, the dominant equations and edge conditions of the theory were obtained. Although their model showed precise predictions of stresses-displacements when collated with other RPTs, it was unable to capture thick plates with SCFC-support order, polynomial functions, and an analytical and 3D approach.

Neglecting the use of shear correction elements connected with FSDTs, Sayyad and Ghugal [37], as well as Ghugal and Gajbhiye [38] captured the effect of shear and strain deformation in their bending study. The phenomenon of zero-shear transverse stresses was satisfactory. Polynomial displacement functions with 3D theory and SCFC plates were not considered in their assessment.

Simply-supported plates under transverse bi-sinusoidal loads were evaluated by Mantari and Soares [39] using the precept of virtual work and HSDT with an assumed variation of the mechanical properties of the plates in the thickness axis. The authors obtained a Navier-type analytical solution which showed a level of accuracy compared to the previous shear deformation model. The 3D theory and polynomial shape functions were not applied. Plates with SCFC edge status were not covered.

Both trigonometric and polynomial displacement functions were employed by Onyeka and Okeke [40] to formulate the governing differential equation for SSFS plates. They used the direct energy method in their bending analysis and the deflection and stresses obtained in their study were in good agreement with the other RPTs. 3-D theory and SCFC plates were not encapsulated in their study. Mantari *et al.* [41] employed trigonometric functions and shear deformation plate theory to obtain the displacement and stresses in thick rectangular plate. The approach applied by the authors cannot be reliable for a thick plate analysis as they cannot give an exact solution. The authors did not apply 3D theory, neither were polynomial functions incorporated. Plates with SSFS support status was not addressed in their study. An alternate refined plate model was developed by Onyeka *et al.,* (2021) [42] for analyzing the effect of bending CCFC thick plates using the energy method. The authors obtained exact solutions as 3-D kinematic and constitutive relations were applied to formulate the equilibrium equations and total energy function. The beauty of their analytical approach and solutions is undeniable but their model was not a blend of the polynomial RPT and the 3D plate theory rather a trigonometric displacement function was used. In addition, plates with SCFC edge status were not considered in their study.

The spline-collocation method with two-coordinate directions and a numerical approach based on the 3-D theory was employed by Grigorenko *et al.,* [43] to get the bending solutions of a thick plate. They determined the displacements-stresses in clamped plates. Their approach did not capture accurately the value for out-of-plane displacements at any given point in the plate. They did not cover plates with the SCFC support - condition. Onyeka *et al.* [1], Onyeka and Mama [44] presented a 3D trigonometric model for CSCS and SSSS plates respectively. The authors solved the bending issue of these plates using a direct variational energy approach. The solutions obtained in their study validate the accuracy of 3D prediction. But a combination of 2D-RPT and 3D theory with the polynomial function were not considered in their study. Plates with the SCFC boundary condition was also not addressed.

The 3-D model was adopted by Hadi *et al.,* [45] to examine the bending characteristics of functionally graded rectangular plates with variable exponential properties. The authors numerically expressed the impact of different functionally-graded inequality on the stress and displacement fields. They presented the exact solutions of the stresses-displacements and the effects of the graded-

material's properties on the plate's behavior, without considering polynomial functions and SCFC isotropic thick rectangular plates.

The study of the behavior of plates using non-classical elasticity theories, have gained more attention in recent times. Many authors have investigated nanostructures using nonlocal elasticity, strain gradient and nonlocal strain gradient theory. Functionally graded material has been the subject of concentration.

These studies include those of Farajpour *et al.* [46], Rahmani *et al.* [47], Shishesaz *et al.* [48], Ebrahimi and Haghi [49], Hosseini *et al.* [50], Nejad and Hadi [51, 52], Nejad *et al.* [53], Farajpour and Rastgoo [54], Farajpour *et al.* [55, 56], Hosseini *et al.* [57], Ebrahimi and Salari [58], Ebrahimi and Barati [59, 60], Hadi *et al.* [61], Asemi and Farajpour [62]. Plate bending features was not considered by these authors, neither was isotropic thick SCFC rectangular plates covered. The 3D elasticity plate theory was also not addressed in their studies. Antecedently, refined plate theories were mostly used by many scholars in the bending investigation of rectangular plates while 3D model was used by few authors as shown in the available literatures. The solutions obtained by those that employed 2D-RPTs were inexact because the stresses along the thickness axis were not analyzed. Previous scholars that used 3D theory unlike the present, applied polynomial displacement-shape functions which made their solutions inexact. This study addressed these research gaps and distinctively presented the coalescence of 3-D trigonometry function which was not seen in preceding studies. The assumed shape functions applied in prior studies birthed erroneous and unreliable solutions as the functions were not derived from the governing compatibility equation that was obtained from the first principle. Close-form solutions, safe and cost-effective analysis is achieved in this work as it employed exact displacement functions in the form of trigonometry.

An exact bending solution for thick plates under uniformly distributed transverse loads with one simply supported edge, one free edge and clamped at the two outer edges (SCFC), is presented in this study using 3-D trigonometric plate theory. Exact trigonometric-displacement-functions were used to determine the variation of displacements and stresses with respect to the aspect ratio in the plate structure.

2. Methodology

2.1 Model Formulation

The model of this study was formulated by considering a rectangular plate in Figure 1 as a three-dimensional element in which the deformation exists in the three axis: length (a), width (b) and thickness (t). The displacement field which includes the displacements along x, y and z-axes: p, q and U are obtained assuming that the x-z section and y-z section, which are initially normal to the x-y plane before bending go off normal to the x-y plane after bending of the plate (see Figure 1).
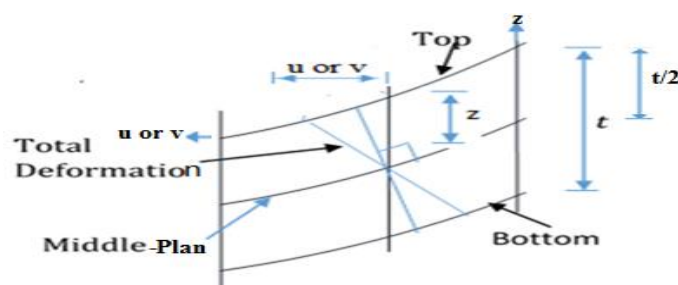
Figure 1: Displacement of x-z (or y-z) section after bending [4]

2.2. Kinematics

The kinematics of the study if formulated by taking the assumption of the plate that the x-z section and y-z section, is no longer normal to the x-y plane after bending. Thus, the 3-D displacement kinematics along x, y and z axis are obtained in line with the work of Onyeka *et al.* [2], as:

$$p = z.\emptyset_x \qquad (1)$$

$$q = z.\emptyset_y \qquad (2)$$

Given that:

$$z = kt \qquad (3)$$

$$\beta = \frac{a}{t} \qquad (4)$$

$$\gamma = \frac{b}{a} \qquad (5)$$

Thus, the six non-dimensional coordinates strain components were derived using strain-displacement expression according to Hooke's law and presented in Equation (6) - (11):

$$\varepsilon_x = \frac{1}{a}.\frac{\partial p}{\partial u} \qquad (6)$$

$$\varepsilon_y = \frac{1}{a\gamma}.\frac{\partial q}{\partial v} \qquad (7)$$

$$\varepsilon_z = \frac{1}{t}.\frac{\partial \cup}{\partial k} \qquad (8)$$

$$\gamma_{xy} = \frac{1}{a}.\frac{\partial q}{\partial u} + \frac{1}{a\gamma}.\frac{\partial p}{\partial v} \qquad (9)$$

$$\gamma_{xz} = \frac{1}{a}.\frac{\partial \cup}{\partial u} + \frac{1}{t}.\frac{\partial p}{\partial k} \qquad (10)$$

$$\gamma_{yz} = \frac{1}{a\gamma}.\frac{\partial \cup}{\partial v} + \frac{1}{t}.\frac{\partial q}{\partial k} \qquad (11)$$

2.3. Constitutive Relations

The three dimensional constitutive relation for isotropic material is given as (see [65]):

$$\begin{bmatrix} \varepsilon_x \\ \varepsilon_y \\ \varepsilon_z \\ \gamma_{xz} \\ \gamma_{yz} \\ \gamma_{xy} \end{bmatrix} = \frac{1}{E} \begin{bmatrix} 1 & -\mu & -\mu & 0 & 0 & 0 \\ -\mu & 1 & -\mu & 0 & 0 & 0 \\ -\mu & -\mu & 1 & 0 & 0 & 0 \\ 0 & 0 & 0 & 2(1+\mu) & 0 & 0 \\ 0 & 0 & 0 & 0 & 2(1+\mu) & 0 \\ 0 & 0 & 0 & 0 & 0 & 2(1+\mu) \end{bmatrix} \begin{bmatrix} \sigma_x \\ \sigma_y \\ \sigma_z \\ \tau_{xz} \\ \tau_{yz} \\ \tau_{xy} \end{bmatrix} \qquad (12)$$

The six stress components were obtained by substituting Equations 6 to 11 into Equation 12 and simplifying the outcome gave:

$$\sigma_x = \left[\mu \frac{kt}{\gamma a} * \frac{\partial \emptyset_y}{\partial v} + (1 - \mu) \frac{kt}{a} * \frac{\partial \emptyset_x}{\partial u} + \mu \frac{1}{t} \right. \left. * \frac{\partial \cup}{\partial k} \right] \frac{E}{(1 + \mu)(1 - 2\mu)} \tag{13}$$

$$\sigma_y = \left[\mu k t * \frac{\partial \emptyset_x}{a \partial u} + \frac{\mu}{t} * \frac{\partial \cup}{\partial k} + \frac{(1 - \mu)kt}{\gamma a} \right. \left. * \frac{\partial \emptyset_y}{\partial v} \right] \frac{E}{(1 + \mu)(1 - 2\mu)} \tag{14}$$

$$\sigma_z = \left[\frac{\mu k t}{\gamma a} * \frac{\partial \emptyset_y}{\partial v} + \frac{(1 - \mu)}{t} * \frac{\partial \cup}{\partial k} + \mu k t \right. \left. * \frac{\partial \emptyset_x}{a \partial u} \right] \frac{E}{(1 + \mu)(1 - 2\mu)} \tag{15}$$

$$\tau_{xy} = \left[\frac{kt \partial \emptyset_y}{a 2 \partial u} * \frac{kt}{2\gamma a} \frac{\partial \emptyset_x}{\partial v} \right] \frac{E(1 - 2\mu)}{(1 + \mu)(1 - 2\mu)} \tag{16}$$

$$\tau_{yz} = \left[\frac{1}{a 2\gamma} \frac{\partial \cup}{\partial Q} + \frac{\emptyset_y}{2} \right] \frac{(1 - 2\mu)E}{(1 + \mu)(1 - 2\mu)} \tag{17}$$

$$\tau_{xz} = \left[\frac{1}{a} \frac{\partial \cup}{2 \partial u} + \frac{\emptyset_x}{2} \right] \frac{(1 - 2\mu)E}{(1 + \mu)(1 - 2\mu)} \tag{18}$$

2.4. Formulation of Energy

The potential energy which is the summation of all the external work done on the body of the material and strain energy generated due to the applied load on the plate is mathematically defined as:

$$\not\exists = \in - \ni \tag{19}$$

Given that;

$$\ni = wab \cap \int_0^1 \int_0^1 \complement \, du \, dv \tag{20}$$

And;

$$\in = \frac{tab}{2} \int_0^1 \int_0^1 \int_{-0.5}^{0.5} \left(\sigma_x \varepsilon_x + \sigma_y \varepsilon_y + \sigma_z \varepsilon_z + \tau_{xy} \gamma_{xy} + \tau_{xz} \gamma_{xz} + \tau_{yz} \gamma_{yz} \right) du \, dv \, dk \tag{21}$$

Substituting Equations 22 and 25 into Equation 24 to get the energy equation as:

$$\not{A} = \frac{Et^3\gamma}{24(1+\mu)(1-2\mu)}\int_0^1\int_0^1\left[\left(\frac{\partial\emptyset_y}{\partial u}\right)^2\frac{(1-2\mu)}{2} + \frac{1}{\gamma}\frac{\partial\emptyset_x}{\partial u}*\frac{\partial\emptyset_y}{\partial v} + \frac{(1-\mu)}{\gamma^2}\left(\frac{\partial\emptyset_y}{\partial v}\right)^2\right. \tag{22}$$

$$+ \frac{(1-\mu)}{t^2}*\left(\frac{\partial\cup}{\partial k}\right)^2\beta^2 + \frac{(1-2\mu)}{2\gamma^2}\left(\frac{\partial\emptyset_x}{\partial v}\right)^2$$

$$+ \frac{6(1-2\mu)}{t^2}\left\{a^2{\emptyset_x}^2 + \left(\frac{\partial\cup}{\partial u}\right)^2 + a^2{\emptyset_y}^2 + \left(\frac{\partial\cup}{\partial v}\right)^2\frac{1}{\gamma^2} + a\left(\frac{\partial\cup}{\partial u}\right)2\emptyset_x\right.$$

$$\left.+ \left(\frac{\partial\cup}{\partial v}\right)2a*\frac{\emptyset_y}{\gamma}\right\} + \left(\frac{\partial\emptyset_x}{\partial u}\right)^2(1-\mu)\bigg]\partial u\partial v - w\gamma a^2\int_0^1\int_0^1 CS\,\partial u\partial v$$

2.5. Solution to the Equilibrium Equation

The two compatibility equations were obtained by minimizing the total potential energy functional with respect to rotations in x-z and in y-z plane to give:

$$\frac{Et^3\gamma}{24(1+\mu)(1-2\mu)}\int_0^1\int_0^1\left[2(1-\mu)\frac{\partial^2\emptyset_x}{\partial u^2} + \frac{\partial^2\emptyset_y}{\partial u\partial v}*\frac{1}{\gamma} + \frac{(1-2\mu)}{\gamma^2}\frac{\partial^2\emptyset_x}{\partial v^2}\right. \tag{23}$$

$$\left.+ \left(2a^2\theta_{sx} + 2a.\frac{\partial\cup}{\partial u}\right)\frac{6(1-2\mu)}{t^2}\right]\partial u\partial v = 0$$

$$\frac{Et^3\gamma}{24(1+\mu)(1-2\mu)}\int_0^1\int_0^1\left[\frac{\partial^2\emptyset_x}{\partial u\partial v}*\frac{1}{\gamma} + 2\frac{\partial^2\emptyset_y}{\partial v^2}*\frac{(1-\mu)}{\gamma^2} + 2\frac{(1-2\mu)}{2}\frac{\partial^2\emptyset_y}{\partial u^2}\right. \tag{24}$$

$$\left.+ \left(2a^2\emptyset_y + \frac{2a.}{\gamma}\frac{\partial\cup}{\partial v}\right)\frac{6(1-2\mu)}{t^2}\right]\partial u\partial v = 0$$

The solution of the equilibrium differential equation gives the characteristics trigonometric displacement and rotation functions as presented in the Equation 25-27 as:

$$\cup = [1\ \ u\ \ Cos\,(uc_1)\ \ Sin\,(uc_1)]\begin{bmatrix}a_0\\a_1\\a_2\\a_3\end{bmatrix}.[1\ \ v\ \ Cos\,(vc_1)\ \ Sin\,(vc_1)]\begin{bmatrix}b_0\\b_1\\b_2\\b_3\end{bmatrix} \tag{25}$$

$$\emptyset_x = \frac{c}{a}.H_0.[1\ \ c_1 Sin\,(uc_1)\ \ c_1 Cos\,(uc_1)]\begin{bmatrix}a_1\\a_2\\a_3\end{bmatrix}.[1\ \ v\ \ Cos\,(vc_1)\ \ Sin\,(vc_1)]\begin{bmatrix}b_0\\b_1\\b_2\\b_3\end{bmatrix} \tag{26}$$

$$\emptyset_y = \frac{c}{a\beta}.H_0.[1\ \ u\ \ Cos\,(uc_1)\ \ Sin\,(uc_1)]\begin{bmatrix}a_0\\a_1\\a_2\\a_3\end{bmatrix}.[1\ \ c_1 Sin\,(vc_1)\ \ c_1 Cos\,(vc_1)]\begin{bmatrix}b_1\\b_2\\b_3\end{bmatrix} \tag{27}$$

Considering a transversely loaded rectangular thick plate whose Poisson's ratio is 0.3 under uniformly distributed load as shown in the Figure 2, the derived trigonometric deflection functions is subjected to a SCFC boundary condition to get the particular solution of the deflection.
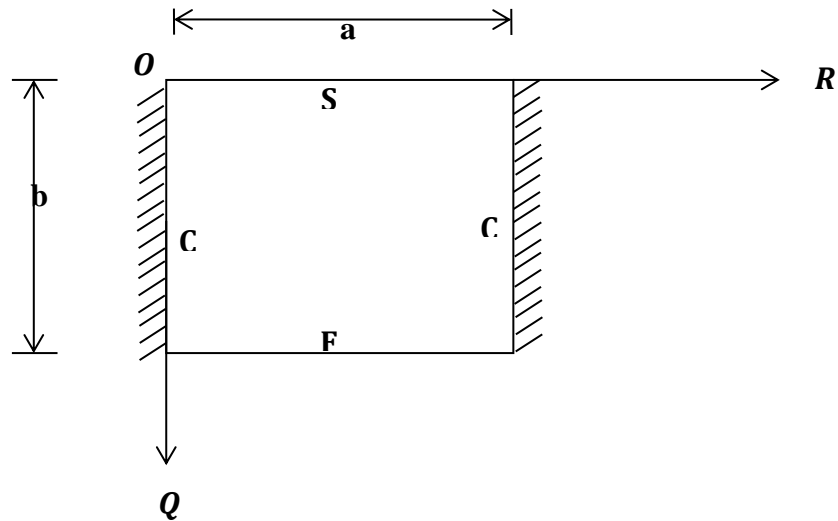
Figure 2: SCFC Rectangular Plate

Applying the initial conditions of the plate in Figure 2, the relationship between the displacement and shape function of the plate as:

$$\cup = C.\cap \tag{28}$$

$$\emptyset_x = \frac{h}{a}.\frac{\partial C}{\partial u} \tag{29}$$

$$\emptyset_y = \frac{g}{\gamma a}.\frac{\partial C}{\partial v} \tag{30}$$

The in trigonometric form of the shape function of the plate after satisfying the boundary conditions is given as:

$$C= (Sin\ \pi u).\left(Cos\frac{\pi v}{2} - 1\right) \tag{31}$$

Substituting Equation 28, 29 and 30 into 22, gives:

$$\nexists = \frac{Et^3\gamma}{24(1+\mu)(1-2\mu)}\Bigg[(1-\mu)h^2 r_x \tag{32}$$
$$+\frac{1}{\gamma^2}\bigg[h.g + \frac{(1-2\mu)h^2}{2} + \frac{(1-2\mu)g^2}{2}\bigg]r_{xy} + \frac{(1-\mu)g^2}{\gamma^4}r_y$$
$$+ 6(1-2\mu)\beta^2\left([h^2 +\cap^2+ 2\cap h].r_z + \frac{1}{\gamma^2}.[g^2 +\cap^2+ 2\cap g].r_{2z}\right)$$
$$-\frac{2qa^4 r_c \cap}{D^*}\Bigg]$$

Where:

$$r_x = \int\limits_0^1 \int\limits_0^1 \left(\frac{\partial^2 C}{\partial u^2}\right)^2 \partial u \partial v \tag{33}$$

$$r_{xy} = \int\limits_0^1 \int\limits_0^1 \left(\frac{\partial^2 C}{\partial u \partial v}\right)^2 \partial u \partial v \tag{34}$$

$$r_y = \int\limits_0^1 \int\limits_0^1 \left(\frac{\partial^2 C}{\partial v^2}\right)^2 \partial u \partial v \tag{35}$$

$$r_z = \int\limits_0^1 \int\limits_0^1 \left(\frac{\partial C}{\partial u}\right)^2 \partial u \partial v \tag{36}$$

$$r_{2z} = \int\limits_0^1 \int\limits_0^1 \left(\frac{\partial C}{\partial v}\right)^2 \partial u \partial v \tag{37}$$

$$r_c = \int\limits_0^1 \int\limits_0^1 C \, \partial u \partial v \tag{38}$$

Minimizing Equation 32 with respect to h gives:

$$\frac{1}{2\gamma^2}[g + h(1 - 2\mu)]r_{xy} + hr_x(1 - \mu) = -6(1 - 2\mu)\beta^2[h + \cap].r_z \tag{39}$$

Minimizing Equation 32 with respect to g gives:

$$\frac{1}{2\gamma^2}[h + g(1 - 2\mu)]r_{xy} + \frac{(1 - \mu)g}{\gamma^4}k_y = +\frac{6}{\gamma^2}(1 - 2\mu)\beta^2([g + \cap].r_{2z}) \tag{40}$$

Re-write the Equation (39) and (40) and simplifying to give:

$$h = \cap \frac{(k_{12}k_{23} - k_{13}k_{22})}{(k_{12}k_{12} - k_{11}k_{22})} \tag{41}$$

$$g = \cap \frac{(k_{12}k_{13} - k_{11}k_{23})}{(k_{12}k_{12} - k_{11}k_{22})} \tag{42}$$

Where;

$$k_{11} = (1 - \mu)r_x + \frac{1}{2\gamma^2}(1 - 2\mu)r_{xy} + 6(1 - 2\mu)\beta^2 r_z \tag{43}$$

$$k_{12} = k_{21} = \frac{1}{2\gamma^2}r_{xy}; \; k_{13} = -6(1 - 2\mu)\beta^2 r_z \tag{44}$$

$$k_{22} = \frac{(1 - \mu)}{\gamma^4}r_y + \frac{1}{2\gamma^2}(1 - 2\mu)r_{xy} + \frac{6}{\gamma^2}(1 - 2\mu)\beta^2 r_{2z} \tag{45}$$

$$k_{23} = k_{32} = -\frac{6}{\gamma^2}(1 - 2\mu)\beta^2 r_{2z} \tag{46}$$

Minimizing Equation 32 with respect to $\cap$ gives:

$$\frac{Et^3\gamma}{24(1+\mu)(1-2\mu)}\left[6(1-2\mu)\beta^2\left([2\cap+2h].r_z+\frac{1}{\gamma^2}.[2\cap+2g].r_{2z}\right)\right]$$
$$-\frac{24wa^4r_c(1+\mu)(1-2\mu)}{Et^3}=0$$

(47)

$$\frac{(1-2\mu)\beta^2Et^3\gamma}{4(1+\mu)(1-2\mu)}\left\{\left[\cap+\cap\frac{(k_{12}k_{23}-k_{13}k_{22})}{(k_{12}k_{12}-k_{11}k_{22})}\right].r_z\right.$$
$$\left.+\frac{1}{\beta^2}.\left[\cap+\cap\frac{(k_{12}k_{13}-k_{11}k_{23})}{(k_{12}k_{12}-k_{11}k_{22})}\right].r_{2z}\right\}$$
$$=\frac{wa^4r_c(1+\mu)(1-2\mu)\beta^3}{E}$$

(48)

Factorizing Equations (48) and simplifying gives:

$$\cap=\frac{2q(1+\mu)(1-2\mu)\beta^3}{E}\left\{\frac{ar_c}{(1-2\mu)\left(\frac{a}{t}\right)^2\left(\left[1+\frac{(k_{12}k_{23}-k_{13}k_{22})}{(k_{12}k_{12}-k_{11}k_{22})}\right].r_z+\frac{1}{\beta^2}.\left[1+\frac{(k_{12}k_{13}-k_{11}k_{23})}{(k_{12}k_{12}-k_{11}k_{22})}\right].r_{2z}\right)}\right\}$$

(49)

2.6. Exact Displacement and Stress Expression

By substituting the value of $\cap$ in Equation 49 into Equation 28, the deflection equation after satisfying the boundary condition of CSFS plate is given as:

$$\cup=\cap(Sin\,\pi u).\left(Cos\frac{\pi v}{2}-1\right)$$

(50)

Similarly, the in-plane displacement along x-axis becomes:

$$p$$

(51)

$$=\frac{(k_{12}k_{23}-k_{13}k_{22})}{(k_{12}k_{12}-k_{11}k_{22})}\left\{\frac{12q(1+\mu)(1-2\mu)\beta^2kr_c}{(1-2\mu)\left(\frac{a}{t}\right)^2\left(\left[1+\frac{(k_{12}k_{23}-k_{13}k_{22})}{(k_{12}k_{12}-k_{11}k_{22})}\right].r_z+\frac{1}{\beta^2}.\left[1+\frac{(k_{12}k_{13}-k_{11})}{(k_{12}k_{12}-k_{11})}\right.}\right.$$

$$p=\frac{12q(1+\mu)(1-2\mu)\beta^2}{E}\left(\frac{kMr_c}{L}\right)\frac{\partial\mathbb{C}}{\partial u}$$

(52)

Where;

$$L=6(1-2\mu)\beta^2\left([1+h].r_z+\frac{1}{\gamma^2}.[1+g].r_{2z}\right)$$

(53)

$$N=\frac{(r_{12}r_{23}-r_{13}r_{22})}{(r_{12}r_{12}-r_{11}r_{22})}$$

(54)

$$M=\frac{(r_{12}r_{13}-r_{11}r_{23})}{(r_{12}r_{12}-r_{11}r_{22})}$$

(55)

Similarly, the in-plane displacement along y-axis becomes;

$$q=\frac{12q(1+\mu)(1-2\mu)\beta}{E}\left(\frac{kNr_c}{L}\right)\frac{\partial\mathbb{C}}{\partial v}$$

(56)

The six stress elements after satisfying the boundary condition are presented in Equations (57) – (62) as:

$$\sigma_x = \frac{E}{(1+\mu)(1-2\mu)}\left[\frac{k}{\beta}\cdot\frac{\partial^2 C}{\partial u^2}(1-\mu)+\mu\beta^4 * \frac{12q(1+\mu)(1-2\mu)}{E}\left(\frac{r_c}{L}\right)\frac{\partial C}{\partial k}\right. \tag{57}$$
$$\left. +\frac{\mu k}{\gamma\beta}\cdot\frac{\partial^2 C}{\partial v^2}\right]$$

$$\sigma_y = \frac{E}{(1+\mu)(1-2\mu)}\left[\frac{\mu k}{\beta}\cdot\frac{\partial^2 C}{\partial u^2}+\mu\beta^4 * \frac{12q(1+\mu)(1-2\mu)}{E}\left(\frac{r_c}{L}\right)\frac{\partial C}{\partial k}\right. \tag{58}$$
$$\left. +\frac{(1-\mu)k}{\gamma\beta}\cdot\frac{\partial^2 C}{\partial v^2}\right]$$

$$\sigma_z = \frac{E}{(1+\mu)(1-2\mu)}\left[\frac{\mu k}{\beta}\cdot\frac{\partial^2 C}{\partial u^2}+(1-\mu)\beta^4 * \frac{12q(1+\mu)(1-2\mu)}{\beta}\left(\frac{r_c}{L}\right)\frac{\partial C}{\partial k}\right. \tag{59}$$
$$\left. +\frac{\mu k}{\gamma\beta}\cdot\frac{\partial^2 C}{\partial v^2}\right]$$

$$\tau_{xy} = \frac{E(1-2\mu)}{(1+\mu)(1-2\mu)}\cdot\left[\frac{k}{2\beta}\cdot\frac{\partial^2\partial C}{\partial u\,\partial v}+\frac{\beta^2 k}{2a\gamma}\cdot\frac{12q(1+\mu)(1-2\mu)}{E}\left(\frac{r_c}{L}\right)\frac{\partial^2\partial C}{\partial u\,\partial v}\right] \tag{60}$$

$$\tau_{xz} = \frac{(1-2\mu)E}{(1+\mu)(1-2\mu)}\cdot\left[\frac{1}{2}\frac{\partial C}{\partial u}+\frac{\beta^3}{2}*\frac{12q(1+\mu)(1-2\mu)}{E}\left(\frac{r_c}{L}\right)\frac{\partial C}{\partial u}\right] \tag{61}$$

$$\tau_{yz} = \frac{(1-2\mu)E}{(1+\mu)(1-2\mu)}\cdot\left[\frac{1}{2}\frac{\partial C}{\partial v}+\frac{\beta^3}{2\gamma}*\frac{12q(1+\mu)(1-2\mu)}{E}\left(\frac{r_c}{L}\right)\frac{\partial C}{\partial v}\right] \tag{62}$$

3. Results and Discussion

This work presents the result of displacements and stresses at span-thickness ratio of 4, 5, 10, 15, 20, 50, 100 and CPT and aspect ratio of length-breadth aspect ratio of 1.0 and 2.0.

The plot in Figures 3 to 4 showed that as the span-depth ratio increased, the out-of-plane displacements (∪) decreased positively while the in-plane displacements (p and q) increased negatively. Table 1 showed that the value of deflection varies more as the span-depth ratio decreases under the same loading capacity/condition. Plates at a span - depth ratio between 4 and 20 can be regarded as thick plates while span-thickness ratio of 50 and beyond can be considered as moderately-thick or thin plates as they are almost equivalent to the value of the CPT. The plate structure tends to fail when the reductions continues to the point where the deflection exceeds the elastic yield stress.

The non-dimensional parameters for the shear stresses in the in the x-y plane (τ_{xy}) increased in the negative order with each rise in the span - depth ratio and the shear stresses in the x-z, and y-z plane (τ_{xz} and τ_{yz}) reduced positively as presented in Figure 9. In Figure 10, there was a negative increase for the shear stresses in the x-y plane (τ_{xy}) for a span - depth ratio of 4 to 5 and 50 to CPT, with a reduction in the positive sense of span-depth ratio of 10 till 20. The same chart revealed the reduction of shear stresses in the x-z plane (τ_{xz}) positively. It also showed a positive reduction for span-depth ratio of 4 to 5, a negative rise in the span - depth ratio of 10 to 20 and a positive decrease for span-thickness ratio of 50 till CPT for shear stresses in the y-z plane (τ_{yz}).

The stresses perpendicular to the x and z axis (σ_x, and σ_z) decreased positively while the ones in the y-axis (σ_y) increased negatively with an increase in span-thickness ratio, as shown in Figure 6. In Figure 3 to 4, the stresses perpendicular to the x-axis (σ_x) reduced positively while stresses perpendicular to the y-axis (σ_y) increased negatively as the span-depth ratio kept rising. Between span-depth ratios of 4 and 5, the normal stress in the z-plane (σ_z) increased negatively, dropped in the negative order at a span - depth ratio of 10 with a gradual negative increment till span-depth ratio of 20 and a constant value at span-depth ratio of 50 and beyond. The normal stresses in the x-axis (σ_x), as shown in Figure 8 decreased in the positive coordinate as the span-thickness ratio increased, perpendicular stresses in the y-axis (σ_y) increased negatively from span-depth ratio of 4 to 15 with a positive increase from span-depth of 20 to CPT. Figure 8 equally showed that stresses perpendicular to the z-axis (σ_z) dropped positively span-depth ratio of 4 and 5, with an increase in the negative sense between span-depth ratio of 10 till 20, maintaining a positive value for span-depth ratio of 50, 100 and CPT.

It can be seen that plates whose deflection and transverse shear stress vary greatly from zero are considered as thick plates while thin plates can be categorized as plates whose vertical shear stress and deflection do not differ largely from zero; their values being almost the same as CPT values. Plates that lie in between the thick and thin plates are considered as moderately-thick plates. Taking a/t to represent the span-thickness ratio for the plate categories; $a/t \geq 40$ are thin plates, $10 \leq a/t \leq 40$ are moderately thick plate, while $a/t \leq 15$ are thick plates. This attestation can be applied to depict the boundary between thin and thick plate. From this study, it can be inferred that thick plate is one whose span-depth ratio value is 4 up to 10.
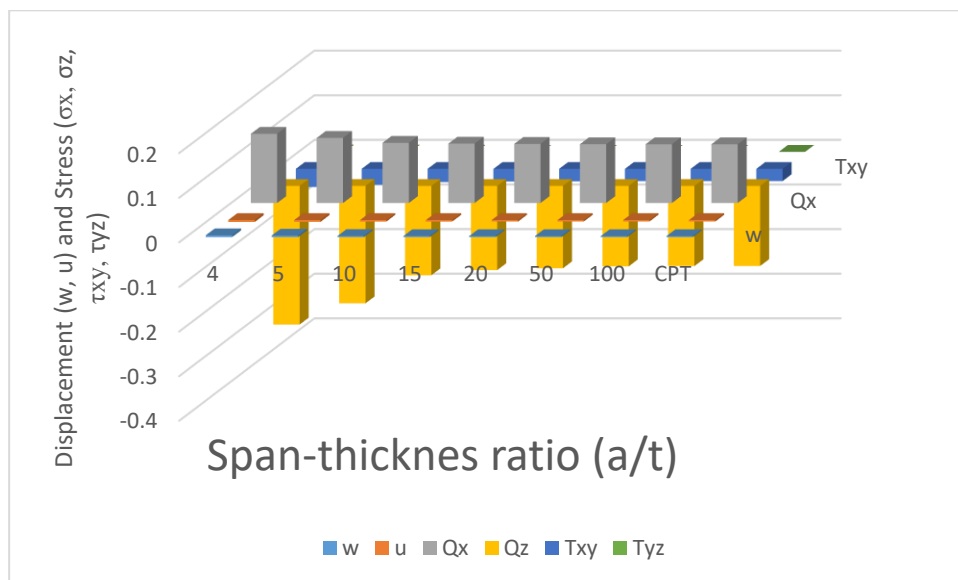
Figure 3: Graph of displacements versus span-depth ratio of the plate at length-breadth ratio of 1.0
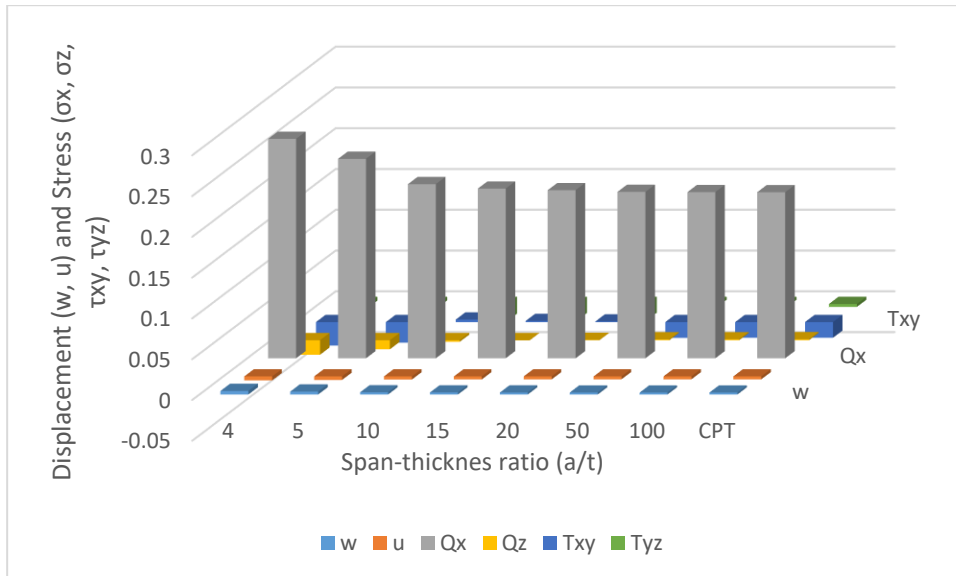
Figure 5: Graph of displacements versus span-depth ratio of the plate at length-breadth ratio of 2.0

The result of the comparative evaluation tabulated in Table 1 and Figure 5 clearly showed the contrariety of this model and those of previous scholars. To validate the derived relationships in the deflection analysis, an assessment of the percentage difference was adopted and recorded in the table. As the span-depth ratio increased, it was observed that the non-dimensional values of deflection for both present and previous studies decreased. The table and the diagram in Figure 12 revealed that the study of [63] varied a little from the present work while that of [64] varied much. The reason for these variations is that [63] employed RPT with an assumed polynomial shape function, while [64] applied a third-order polynomial shear deformation theory with a derived shape function. Significantly, both previous studies did not apply the amalgam of 3-D elasticity plate theory and fourth-order polynomial shear-deformation theory; a feat documented in this work.

Table 1 and Figure 12 revealed the over-estimation and underestimation of the RPT-solutions obtained by previous researchers. This confirms the reliability of this model and the approach considered herein as it gives accurate and exact solutions. This model is worth adopting for safe, cost-effective and accurate analysis of thick plates of any boundary condition. The average percentage difference obtained in this work and [64] is 8.75%, while that of [63] is 5.67%. The overall percentage variation is 8.05%. This implies that the present study can be used in confidence as it is equivalent to those of [64] and [63] at 91.3% and 94.3% confidence level.

Table 1: Comparative deflection analysis of square plate between present studies and past studies at different span-depth ratio

β = a/t	Present Work [P.W]	Onyeka and Okeke (2020) [64]	Gwarah (2019) [63]	Percentage difference between [P.W] & [64]	Percentage difference between [P.W] & [63]
4	0.00407	0.004465	0.003713	9.70516	8.7715
5	0.00340	0.003726	0.003147	9.58824	7.44118
10	0.00253	0.002786	0.002381	10.1186	5.88933
15	0.00238	0.002570	0.002238	7.98319	5.68966
20	0.00232	0.002559	0.002188	10.3017	5.99119
50	0.00227	0.002496	0.002134	9.95595	5.9292

100	0.00226	0.002487	0.002126	10.0442	5.64444
CPT	0.00225	0.002482	0.002123	10.3111	8.7715
Average Percentage difference				8.75	5.67
Total Percentage difference				7.21%	
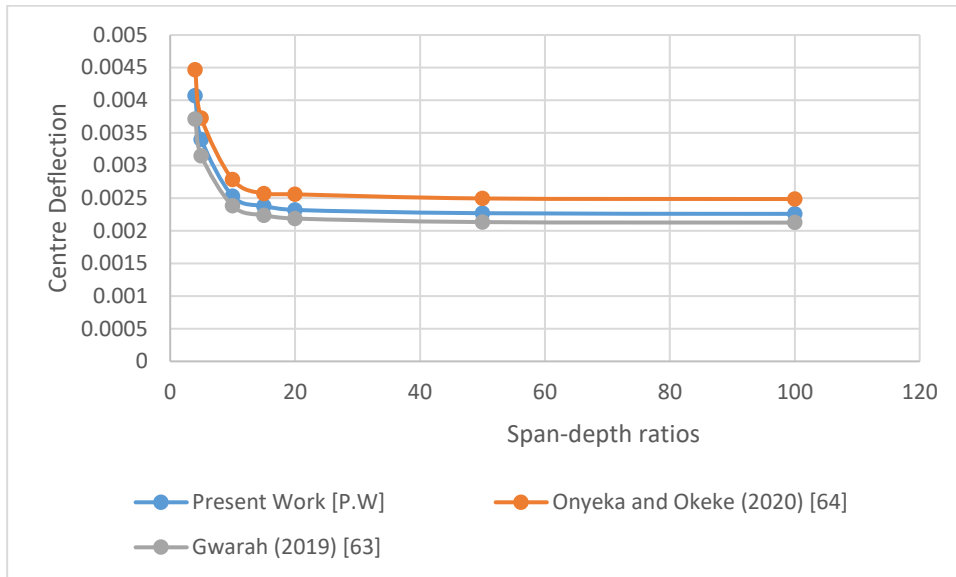
Figure 12: Comparative variation of deflection and span-depth ratios of present study and previous studies

4. Conclusion

A trigonometric 3-d shape function of 3-d was applied for displacements and stresses analysis of shear deformable plate under distributed lateral loading, from which the following conclusions were drawn:

- The exact polynomial displacement functions offered close-form solution
- The application of a 3-D plate equivalence predicts a more reliable solution considering various numerical comparable results and thereby recommended for accurate plate analysis.
- The established formulas in this work can be adopted in the analysis of various categories of plates.

233

Nomenclature

k	non-dimensional parameters of z-axis
u	non-dimensional parameters of x-axis
v	non-dimensional parameters of y-axis
t	thickness of the plate,
p	in-plane displacement along x-axis
q	in-plane displacement along y-axis
h	coefficient of shear deformation along x-axis of the plate
g	coefficient of shear deformation along y-axis of the plate
ε_x	normal strain along x-axis
ε_y	normal strain along y-axis
ε_z	normal strain along z-axis
γ_{xy}	shear strain in the plane parallel to the x-y plane
γ_{xz}	shear strain in the plane parallel to the x-z plane
γ_{yz}	shear strain in the plane parallel to the y-z plane
τ_{xy}	shear stress in the plane parallel to the x-y plane
τ_{xz}	shear stress in the plane parallel to the x-z plane
τ_{yz}	shear stress in the plane parallel to the y-z plane
E	modulus of elasticity
μ	Poisson's ratio
∄	Potential energy of the plate
∈	Strain energy of the plate
∋	External work done on the plate
⊂	Plate's shape function
w	Uniformly distributed load
∪	Deflection function of the plate
∩	Coefficient of deflection
$\emptyset_x$	Coefficient of shear deformation along x-axis
$\emptyset_y$	Coefficient of shear deformation along y-axis
p	In-plane displacement along x-axis
q	In-plane displacement along y-axis
β	Span-thickness ratio
α	Aspect ratio

References

[1] F. C. Onyeka, B. O. Mama and C. D. Nwa-David (2022). Application of Variation Method in Three-Dimensional Stability Analysis of Rectangular Plate Using Various Exact Shape Functions. Nigerian Journal of Technology (NIJOTECH), Vol. 41, no. 1, pp. 8-20. DOI: http://dx.doi.org/10.4314/njt.v41i1.2.

[2] K. Chandrashekhara (2001). Theory of plates. University Press (India) Limited.

[3] I. C. Onyechere, O. M. Ibearugbulem, C. U. Anya, K. O. Njoku, A. U. Igbojiaku and L. S. Gwarah (2020). The Use of Polynomial Deflection Function in The Analysis of Thick Plates using Higher Order Shear Deformation Theory. Saudi Journal of Civil Engineering, Vol.4, no.4, pp. 38-46. DOI: 10.36348/sjce. 2020. v04i04.001.

[4] F. C. Onyeka, B. O. Mama, C. D. Nwa-David and T. E. Okeke (2022). Exact Analytic Solution for Static Bending of 3-D Plate under Transverse Loading. Journal of Computational Applied Mechanics, Vol. 53, No. 3, pp. 309-331. DOI: 10.22059/jcamech.2022.342953.721.

[5] F. C. Onyeka, C. D. Nwa-David and E. E. Arinze (2021). Structural Imposed Load Analysis of Isotropic Rectangular Plate Carrying a Uniformly Distributed Load Using Refined Shear Plate Theory. FUOYE Journal of Engineering and Technology (FUOYEJET), Vol.6, no. 4, pp. 414-419. DOI: http://dx.doi.org/10.46792/fuoyejet.v6i4.719.

[6] J. N. Reddy (2006). Classical theory of plates, In Theory and Analysis of Elastic Plates and Shells, CRC Press. DOI: 10.1201/9780849384165-7

[7] F. C. Onyeka and T. E. Okeke (2020). Application of Higher Order Shear Deformation Theory in The Analysis of Thick Rectangular Plate. International Journal of Emerging Technologies, Vol. 11, no. 5, pp. 62-67.

[8] R. Szilard (2004). Theories and Applications of Plates Analysis: Classical, Numerical and Engineering Methods. John Wiley and Sons Inc. DOI: 10.1002/9780470172872.

[9]   E. Ventsel and T. Krauthammer (2001). Thin plates and shells theory, analysis and applications, Maxwell Publishers Inc, New York.

[10] F. C. Onyeka, T. E. Okeke and C. D. Nwa-David (2022). Static and Buckling Analysis of a Three-Dimensional (3-D) Rectangular Thick Plates Using Exact Polynomial Displacement Function. European Journal of Engineering and Technology Research, Vol. 7, no. 2, pp.29-35. DOI: http://dx.doi.org/10.24018/ejeng.2022.7.2.2725.

[11] F. C. Onyeka, B. O. Mama and C. D. Nwa-David (2022). Analytical Modelling of a Three-Dimensional (3D) Rectangular Plate Using the Exact Solution Approach. IOSR Journal of Mechanical and Civil Engineering (IOSR-JMCE), Vol.19, no. 1, pp. 76-88. DOI: 10.9790/1684-1901017688.

[12] F. C. Onyeka, F. O. Okafor and H. N. Onah (2021). Buckling Solution of a Three-Dimensional Clamped Rectangular Thick Plate Using Direct Variational Method. IOSR Journal of Mechanical and Civil Engineering (IOSRJMCE), Vol. 18, no.3, pp.10-22. DOI: 10.9790/1684-1803031022.

[13] S. P. Timoshenko and J. M. Gere (1963). Theory of elastic stability, 2nd Edition, McGraw-Hill Books Company, New York. DOI: 10.1115/1.3636481.

[14] F. C. Onyeka (2020). Critical Lateral Load Analysis of Rectangular Plate Considering Shear Deformation Effect. Global Journal of Civil Engineering, Vol. 1, pp. 16-27. DOI: 10.37516/global.j.civ.eng.2020.012.

[15] F. C Onyeka and T. E Okeke (2021). Analytical Solution of Thick Rectangular Plate with Clamped and Free Support Boundary Condition using Polynomial Shear Deformation Theory. Advances in Science, Technology and Engineering Systems Journal, Vol.6, no. 1, pp. 1427-1439. DOI: 10.25046/aj0601162.

[16] P. S. Gujar and K. B. (2015). Ladhane, Bending Analysis of simply supported and clamped circular plate. International Journal of Civil Engineering (SSRG-IJCE), Vol. 2, no. 5, pp. 45-51. DOI: 10.14445/23488352/IJCE-V2I5P112.

[17] F. C. Onyeka (2021). Effect of Stress and Load Distribution Analysis on an Isotropic Rectangular Plate. Arid Zone Journal of Engineering, Technology and Environment, Vol. 17, no. 1, pp. 9-26.

[18] F. C. Onyeka and T. E. Okeke (2021). Analysis of critical imposed load of plate using variational calculus. Journal of Advances in Science and Engineering Vol. 4, no. 1, pp. 13–23. DOI: https://doi.org/10.37121/jase.v4i1.125.

[19] E. Reissner (1945). The Effect of Transverse Shear Deformation on the Bending of Elastic Plates. Journal of Applied Mechanics, Vol. 12, no. 2, pp. A69–A77. DOI:10.1115/1.4009435.

[20] M. Zenkour (2003). Ashraf, Exact Mixed-Classical Solutions for the Bending Analysis of Shear Deformable Rectangular Plates. Applied Mathematical Modelling, Vol. 27, no. 7, pp. 515-34. DOI: 10.1016/S0307-904X(03)00046-5.

[21] F. C. Onyeka, F. O. Okafor and H. N. Onah (2021). Application of a New Trigonometric Theory in the Buckling Analysis of Three-Dimensional Thick Plate. International Journal of Emerging Technologies, Vol. 12, no. 1, pp. 228-240.

[22] Y. M. Ghugal and A. S. Sayyad (2011). Free vibration of thick isotropic plates using trigonometric shear deformation theory. J. Solid Mech, Vol. 3, no. 2, pp. 172-182.

[23] A. S. Sayyad and Y. M. Ghugal (2012). Bending and Free Vibration Analysis of Thick Isotropic Plates by Using Exponential Shear Deformation Theory. Applied and Computational Mechanics, Vol. 6, no. 1, pp. 65-82, 2012.

[24] F. C. Onyeka and D. Osegbowa (2020). Stress analysis of thick rectangular plate using higher order polynomial shear deformation theory, FUTO Journal Series-FUTOJNLS, Vol. 6, no. 2, pp. 142-161.

[25] I. I. Sayyad (2013). Bending and Free Vibration Analysis of Isotropic Plate Using Refined Plate Theory. Bonfring International Journal of Industrial Engineering and Management Science, Vol. 3, no. 2, pp. 40-46. DOI:10.9756/bijiems.4390.

[26] O. M. Ibearugbulem and F. C. Onyeka (2020). Moment and Stress Analysis Solutions of Clamped Rectangular Thick Plate. European Journal of Engineering Research and Science, Vol. 5, no. 4, pp. 531-534. DOI:10.24018/ejers.2020.5.4.1898.

[27] G. Kirchhoff (1850). Ueber Die Schwingungen Einer Kreisförmigen Elastischen Scheibe. Annalen Der Physik, Vol. 157, no.10, pp. 258-64. DOI:10.1002/andp.18501571005.

[28] F. C. Onyeka, T. E. Okeke and C. D. Nwa-David (2022). Buckling Analysis of a Three-Dimensional Rectangular Plates Material Based on Exact Trigonometric Plate Theory. Journal of Engineering Research and Sciences, Vol. 1, no. 3, pp. 106-115. DOI: https://dx.doi.org/10.55708/js0103011.

[29] F. C. Onyeka, B. O. Mama and T. E. Okeke (2022). Exact three-dimensional stability analysis of plate using a direct variational energy method. Civil Engineering Journal, Vol. 8, no. 1, pp. 60-80. DOI: http://dx.doi.org/10.28991/CEJ-2022-08-01-05.

[30] M. Kashtalyan (2004). Three-dimensional elasticity solution for bending of functionally graded rectangular plates. European Journal of Mechanics A/Solids, Vol. 23, no. 5, pp. 853-864.

[31] F. C. Onyeka, D. Osegbowa and E. E. Arinze (2020). Application of a New Refined Shear Deformation Theory for the Analysis of Thick Rectangular Plates. Nigerian Research Journal of Engineering and Environmental Sciences, Vol. 5, no. 2, pp. 901-917.

[32] B. O. Mama, C. U. Nwoji, C. C. Ike and H. N. Onah (2017). Analysis of Simply Supported Rectangular Kirchhoff Plates by the Finite Fourier Sine Transform Method. International Journal of Advanced Engineering Research and Science (IJAERS), Vol. 4, no. 3, pp. 285-291. DOI https://doi.org/10.22161/ijaers.4.3.44.

[33] C. U. Nwoji, B. O Mama, C. C Ike and H. N. Onah (2017). Galerkin-Vlasov method for the flexural analysis of rectangular Kirchhoff plates with clamped and simply supported edges. IOSR Journal of Mechanical and Civil Engineering (IOSR JMCE), Vol. 14, no. 2, pp. 61-74. DOI: https://doi.org/10.9790/1684-1402016174.

[34] N. N. Osadebe, C. C. Ike, H. N. Onah, C. U. Nwoji and F. O. Okafor (2016). Application of Galerkin-Vlasov Method to the Flexural Analysis of Simply Supported Rectangular Kirchhoff Plates under Uniform Loads. Nigerian Journal of Technology (NIJOTECH), Vol. 35, no. 4, pp. 732-738. DOI: https://doi.org/10.4314/njt.v35i4.7.

[35] N. G. Iyengar (1988). Structural Stability of Columns and Plates, New York: Ellis Horwood Limited; 1988.

[36] D. P. Bhaskar, A. G. Thakur, I. I. Sayyad and S. V. Bhaskar (2021). Numerical Analysis of Thick Isotropic and Transversely Isotropic Plates in Bending using FE Based New Inverse Shear Deformation Theory. International Journal of Automotive and Mechanical Engineering (IJAME), Vol.18, no. 3, pp. 8882-8894. DOI: https://doi.org/10.15282/ijame.18.3.2021.04.0681.

[37] A. S. Sayyad and Y. M. Ghugal (2012). Bending and free vibration analysis of thick isotropic plates by using exponential shear deformation theory. Applied and Computational Mechanics, Vol. 6, pp. 65-82.

[38] Y. M. Ghugal and P. D. Gajbhiye (2016). Bending Analysis of Thick Isotropic Plates by Using 5th Order Shear Deformation Theory. Journal of Applied and Computational Mechanics, Vol. 2, no. 2, pp. 80-95. DOI: 10.22055/jacm.2016.12366.

[39] J. L. Mantari and C. G. Soares (2012). Bending Analysis of Thick Exponentially Graded Plates Using A New Trigonometric Higher Order Shear Deformation Theory. Composite Structures, Vol. 94, no. 6, pp. 1991-2000. DOI: https://doi.org/10.1016/j.compstruct.2012.01.005.

[40] F. C. Onyeka and T. E. Okeke (2021). New Refined Shear Deformation Theory Effect on Non-Linear Analysis of a Thick Plate Using Energy Method. Arid Zone Journal of Engineering, Technology & Environment, Vol. 17, no. 1, pp.121-140.

[41] J. L. Mantari, A. S. Oktem, C. Guedes Soares (2012). A New Trigonometric Shear Deformation Theory for Isotropic, Laminated Composite and Sandwich Plates. International Journal of Solids and Structures, Vol. 49, no. 1, pp. 43-53. DOI: http://doi.org/10.1016/j.ijsolstr.2011.09.008.

[42] F. C. Onyeka, B. O. Mama and T. E. Okeke (2021). Elastic Bending Analysis Exact Solution of Plate using Alternative I Refined Plate Theory. Nigerian Journal of Technology (NIJOTECH), Vol. 40, no. 6, pp. 1018-1029. DOI: http://dx.doi.org/10.4314/njt.v40i6.4.

[43] A.Y. Grigorenko, A. S. Bergulev, S. N. Yaremchenko (2013). Numerical solution of bending problems for rectangular plates. International Applied Mechanics, Vol. 49, no.1, pp.81-94. DOI: https://doi.org/10.1007/s10778-013-0554-1.

[44] F. C. Onyeka and B. O. Mama (2021). Analytical Study of Bending Characteristics of an Elastic Rectangular Plate using Direct Variational Energy Approach with Trigonometric Function. Emerging Science Journal, Vol. 5, No. 6, pp. 916-928. DOI: http://dx.doi.org/10.28991/esj-2021-01320.

[45] A. Hadi, A. Rastgoo, A. Daneshmehr and F. Ehsani (2013). Stress and strain analysis of functionally graded rectangular plate with exponentially varying properties. Indian Journal of Materials Science, Vol. 2013, 2013.

[46] M. R. Farajpour, A. Rastgoo, A. Farajpour and M. Mohammadi (2016). Vibration of piezoelectric nanofilm-based electromechanical sensors via higher-order non-local strain gradient theory. Micro. Nano Lett., Vol. 11, no. 6, pp. 302-307. DOI: https://doi.org/10.1049/mnl.2016.0081.

[47] O. Rahmani, S. Norouzi, H. Golmohammadi and S. Hosseini (2017). Dynamic response of a double, single-walled carbon nanotube under a moving nanoparticle based on modified nonlocal elasticity theory considering surface effects. Mech. Adv. Mater. Struct., Vol. 24, no. 15, pp. 1274-1291. DOI: https://doi.org/10.1080/15376494.2016.1227504.

[48] M. Shishesaz, M. Hosseini, K. N Tahan and A. Hadi (2017). Analysis of functionally graded nanodisks under thermoelastic loading based on the strain gradient theory. Acta Mechanica, Vol. 228, no. 12, pp. 4141-4168. DOI: https://doi.org/10.1007/s00707-017-1939-8.

[49] F. Ebrahimi and P. Haghi (2018). Elastic wave dispersion modelling within rotating functionally graded nanobeams in thermal environment. Adv. Nano Res., Int. J., Vol. 6, no. 3, pp. 201-217. DOI: https://doi.org/10.12989/anr.2018.6.3.201.

[50] M. Hosseini, M. Shishesaz, K. N. Tahan and A. Hadi (2016). Stress analysis of rotating nano-disks of variable thickness made of functionally graded materials. Int. J. Eng. Sci., Vol. 109, pp. 29-53. DOI: https://doi.org/10.1016/j.ijengsci.2016.09.002.

[51] M. Z. Nejad, A. Hadi (2016). Eringen's non-local elasticity theory for bending analysis of bi-directional functionally graded Euler–Bernoulli nano-beams. Int. J. Eng. Sci., Vol. 106, pp. 1-9. DOI: https://doi.org/10.1016/j.ijengsci.2016.05.005

[52] M. Z. Nejad, A. Hadi (2016). Non-local analysis of free vibration of bi-directional functionally graded Euler–Bernoulli nano-beams. Int. J. Eng. Sci., vol. 105, pp. 1-11. DOI: https://doi.org/10.1016/j.ijengsci.2016.04.011

[53] M. Z. Nejad, A. Hadi and A. Rastgoo (2016). Buckling analysis of arbitrary two-directional functionally graded Euler–Bernoulli nano-beams based on nonlocal elasticity theory. Int. J. Eng. Sci., Vol. 103, pp. 1-10. DOI: https://doi.org/10.1016/j.ijengsci.2016.03.001

[54] A. Farajpour and A. Rastgoo (2017). Influence of carbon nanotubes on the buckling of microtubule bundles in viscoelastic cytoplasm using nonlocal strain gradient theory. Results Phys., Vol. 7, pp. 1367-1375. DOI: https://doi.org/10.1016/j.rinp.2017.03.038

[55] A. Farajpour, A. Rastgoo and M. Farajpour (2017). Nonlinear buckling analysis of magneto-electro-elastic CNT-MT hybrid nanoshells based on the nonlocal continuum mechanics. Compos. Struct., Vol. 180, pp.179-191. DOI: https://doi.org/10.1016/j.compstruct.2017.07.100

[56] A. Farajpour, A. Rastgoo and M. Mohammadi (2017). Vibration, buckling and smart control of microtubules using piezoelectric nanoshells under electric voltage in thermal environment. Physica B: Condensed Matter, Vol. 509, pp. 100-114. DOI: https://doi.org/10.1016/j.physb.2017.01.006

[57] M. Hosseini, H. H Gorgani, M. Shishesaz, A. Hadi (2017). Size-dependent stress analysis of single-wall carbon nanotube based on strain gradient theory. Int. J. Appl. Mech., vol.9, no. 6. DOI: https://doi.org/10.1142/S1758825117500879

[58] F. Ebrahimi, P. Haghi (2018). Elastic wave dispersion modelling within rotating functionally graded nanobeams in thermal environment. Adv. Nano Res., Int. J., Vol. 6, no. 3, pp. 201-217. DOI: https://doi.org/10.12989/anr.2018.6.3.201

[59] F. Ebrahimi and M. R. Barati (2018). Buckling Analysis of nonlocal strain gradient axially functionally graded nanobeams resting on variable elastic medium. Proc. Inst. Mech. Eng. Pt. C J. Mech. Eng. Sci., Vol. 232, no. 11, pp. 2067-2078. DOI: https://doi.org/10.1177/0954406217713518.

[60] F. Ebrahimi and M. R. Barati (2018). Stability analysis of functionally graded heterogeneous piezoelectric nanobeams based on nonlocal elasticity theory. Adv. Nano Res., Int. J., vol. 6, no. 2, pp. 93-112. DOI: https://doi.org/10.12989/anr.2018.6.2.093.

[61] A. Hadi, M. Z Nejad, M. Hosseini (2018). Vibrations of three-dimensionally graded nanobeams. Int. J. Mech. Sci., Vol. 128, pp. 12-23. DOI: https://doi.org/10.1016/j.ijengsci.2018.03.004.

[62] S. R. Asemi, A. Farajpour (2014). Vibration Characteristics of double-piezoelectric-nanoplate-systems. Micro. Nano Lett., Vol. 9, no. 4, pp. 280-285. DOI: https://doi.org/10.1049/mnl.2013.0741.

[63] L. S. Gwarah (2019). Application of shear deformation theory in the analysis of thick rectangular plates using polynomial displacement functions. PhD Thesis Presented to the School of Civil Engineering, Federal University of Technology, Owerri, Nigeria.

[64] F. C. Onyeka and T. E Okeke (2020). Effect of load, shear and bending analysis of rectangular plate using polynomial displacement function. Journal of Research and Innovations in Engineering, Vol. 5, pp. 145-158.

[65] T. E. Okeke, F. C. Onyeka and C. D. Nwa-David (2022). Characteristic Trigonometric Function Application to the Direct Variation Method for Clamped, Simply and Freely Supported Plate under Uniform Load Distributions. Journal of Materials Engineering, Structures and Computation, Vol.1, no. 1, pp. 40-58, 2022.